Release of gaseous and particulate carbonaceous compounds from biomass burning during the SAFARI 2000 dry season field campaign

C. Hély, K. Caylor, S. Alleaume, R. J. Swap, and H. H. Shugart
Environmental Sciences Department, University of Virginia, Charlottesville, Virginia, USA

Received 26 April 2002; revised 18 September 2002; accepted 2 October 2002; published 13 February 2003.

[1] Source strengths to the atmosphere for different forms of carbon (CO_2, CO, CH_4, nonmethane hydrocarbons (NMHC), and $PM_{2.5}$) produced by biomass burning were calculated during the Southern African Regional Science Initiative (SAFARI 2000) intensive study period (August and September 2000) for Africa south of the equator. For a given pixel burned, these calculations are a product of the aboveground biomass before a fire, the proportion of biomass that is burned by the fire, and the emission factor for a given carbon compound based on the combustion efficiency. The total emission for the region is the summation of such calculations for all the burned pixels. Products used for these calculations are a prototype satellite-based burned area based on the SPOT-VGT-S1 satellite product, a fuel load map produced by a simulation model developed and applied to southern Africa at 1 km^2 resolution, information from fire experiments from our own research in southern Africa to compute combustion completeness, and emission factors published for the region. Over August and September 2000, 31,067 fires detected by the SPOT satellite are calculated to have emitted 96.9×10^{12} g CO_2, 4.6×10^{12} g CO, and lesser amounts of CH_4, NMHC, and $PM_{2.5}$. These calculations are in the range of previous estimates of the emissions of these compounds for southern Africa. Along with documenting the estimates of the emissions during the SAFARI 2000 campaign, regional emission estimates are very strongly controlled by the burned area of fires due to a correlation between the cumulative distribution of percent burned area and the cumulative distribution of percent emissions. *INDEX TERMS:* 0305 Atmospheric Composition and Structure: Aerosols and particles (0345, 4801); 1615 Global Change: Biogeochemical processes (4805); 9305 Information Related to Geographic Region: Africa; *KEYWORDS:* area burned, regional fuel load, combustion completeness, combustion efficiency, emission factors, emissions

Citation: Hély, C., K. Caylor, S. Alleaume, R. J. Swap, and H. H. Shugart, Release of gaseous and particulate carbonaceous compounds from biomass burning during the SAFARI 2000 dry season field campaign, *J. Geophys. Res.*, *108*(D13), 8470, doi:10.1029/2002JD002482, 2003.

1. Introduction

[2] Biomass burning is generally considered to be a primary source of aerosols and trace gases emitted annually in subequatorial Africa [*Fishman et al.*, 1991; *Pickering et al.*, 1994; *Andreae*, 1995]. Several major field investigations, SAFARI-92/TRACE-A [*Lindesay et al.*, 1996], BHATTEX [*Piketh et al.*, 1999], and most recently Southern African Regional Science Initiative (SAFARI 2000), have attempted to improve estimates of aerosol and trace gas emissions derived from biomass burning in southern Africa. These investigations have suggested that uncertainties in emission from biomass burning were mainly due to the use of available biomass estimates based only on qualitative vegetation descriptions, as well as high variability in the estimates of burned area at regional scales over time. A major objective of the recently conducted SAFARI 2000 is the determination of regional emissions of trace gases and aerosols from biomass burning, biogenic, mineral and industrial sources [*Swap et al.*, 2002a].

[3] As part of SAFARI 2000, several intensive field campaigns during both the southern African wet and dry seasons were conducted [*Swap et al.*, 2002b; *Otter et al.*, 2002]. This paper provides biomass burning emission estimates for continental Africa south of the equator during the SAFARI 2000 Dry Season Intensive conducted during August and September 2000. In addition, we describe the methodology used to improve parameterizations of regional fuel load and combustion completeness. Available burned area products and emission factors are used to produce an estimate of emissions derived from regional biomass burning for the region during the months of August and September 2000. The contribution of cumulative emissions by fire size is explored, and a relationship between burned area and total emissions during the SAFARI 2000 Dry Season Intensive is derived for the region. The estimates

0148-0227/03/2002JD002482

and the uncertainties associated with their determination are placed in the context of SAFARI 2000.

2. Methodology

[4] This study employs a nested approach to determine regional emissions. Ground-based observations of fuel characterization and combustion completeness are coupled with fuel load modeling and remotely sensed products of vegetation structure, and burned area. These data are used to estimate emissions of the gaseous compounds CO_2, CO, CH_4, and nonmethane hydrocarbons (NMHC) as well as particulate matter less than 2.5 μm in diameter ($PM_{2.5}$) for the region. Although the formation of elemental carbon ash can constitute a significant portion of fire product [*Kuhlbusch et al.*, 1996], we do not provide estimates of carbon ash formation due to a lack of proven regional-scale modeling approaches for these compounds. Monthly estimates of potential compound-specific emissions during the months of August and September for each 1 km^2 pixel $[i, j]$ are calculated using the following equation:

$$[E_x]_{ij} = [F]_{ij} \times [CC]_{ij} \times [EF_x]_{ij} \quad (1)$$

where:

E_x Potential emissions released for compound x [g km^{-2}]
F Prefire aboveground fuel load (dry matter) [kg DM km^{-2}]
CC Combustion completeness [%]
EF_x Emission factor for compound x [g compound kg^{-1} DM]

[5] The resulting matrix is a 3901 × 4201 array of potential emission estimates at each 1 km^2 pixel for every compound considered. Total regional emission of each compound ($E_x total$ [g compound]) during the intensive study period is found by summing the product of potential emissions estimates and the value of the burned area occurrence in each pixel (0 or 1) according to (2).

$$E_x total = \sum \left([E_x]_{ij} \times [A]_{ij} \right) \quad (2)$$

where:

A Burned area occurrence, either 0 or 1 for the current month.

[6] It is important to distinguish the difference between "fuel load" (F), "biomass burned," and "carbon burned" in order to maintain mass balance between available fuel and fire emissions. Following (1), the total biomass burned (B [kg DM km^{-2}]) in pixel $[i,j]$ is the product of available fuel (F) and combustion completeness (CC), or proportion of fuel that is burned, according to (3).

$$[B]_{ij} = [F]_{ij} \times [CC]_{ij} \quad (3)$$

[7] Subsequently, the mass of carbon consumed within a pixel (M_C [kg C km^{-2}]) is determined from (4).

$$[M_C]_{ij} = [B]_{ij} \times 0.45 \quad (4)$$

where:

0.45 Proportion of Carbon per unit biomass fuel [g C (g DM^{-1})], generally taken to be 0.45 [*Scholes and Walker*, 1993] and varying between 0.4 and 0.5 [*Crutzen and Andreae*, 1990; *Prince et al.*, 1995].

[8] At each pixel, we define the sum of emitted carbon as E_C [g C km^{-2}], which is found using the ratio of carbon mass to molecular weight in each emission compound (Mr), as in (5). In this study, we are using values of 0.2727, 0.4286, 0.7500, 0.8000, and 0.4000 for Mr_{CO_2}, Mr_{CO}, Mr_{CH_4}, Mr_{NMCH}, and $Mr_{PM_{2.5}}$ respectively. Values of Mr_{NMCH}, and $Mr_{PM_{2.5}}$ are estimated using the lowest possible ratio of carbon mass to molecular weight for NMHC and estimates of carbon content in fine particulate matter (Macko, personal communication).

$$[E_C]_{ij} = \sum_x [E_x]_{ij} \times Mr_x \quad (5)$$

[9] It is apparent that the total emissions of carbon-bearing compounds must be constrained by M_C, so that the relationship in (6) is true for all pixels $[i,j]$.

$$\frac{[E_C]_{ij}}{[M_c]_{ij}} \leq 1 \quad (6)$$

Substitution for E_C and M_C according to (5), (4), and (3) yields (7), which shows the constraint of emission estimates of carbon (g C) on total carbon in fuel (450 g C per kg fuel).

$$\frac{\sum [EF_x]_{ij} \cdot Mr_x}{450} \leq 1 \quad (7)$$

[10] In this study, we are following the approach of previous studies by only estimating the emission of the 5 most important carbonaceous compounds. In addition, we are not predicting carbon ash formation. Therefore, because all carbonaceous compounds are not accounted for in the modeled emissions estimates, it is possible that (7) may be less than 1. The products used to estimate the various terms in (1)–(7) and how they vary from earlier approaches [*Scholes et al.*, 1996a, 1996b; *Hao et al.*, 1996] are described in the following sections.

2.1. Area Burned Product (A)

[11] This study uses the recently released prototype of Global Burnt Area 2000 produced by the Global Burnt Area 2000 Initiative (GBA2000) developed by the Global Vegetation Monitoring unit [*Grégoire et al.*, 2002] at the Joint Research Centre of the European Commission. This data set has been derived from a daily time series of medium-resolution (1 km^2) satellite imagery provided by the SPOT-VGT-S1 (J.-M. Grégoire and K. Tansey, The GBA2000 initiative: Developing a global burned area database from SPOT-VEGETATION imagery, submitted to *International Journal of Remote Sensing*, 2002). The burnt area detection algorithm developed is based on a classification tree approach [*Pereira et al.*, 2000]. The algorithm uses the spectral response of burnt areas in the visible, near infrared, middle infrared and thermal infrared as well as vegetation indices to define burned areas. Although thermal

infrared is used in the algorithm, active fire detection is not used determine burned pixels.

[12] The subset of burned area occurrence provides monthly total area burned over the region with a 1 km^2 spatial resolution. The GBA2000 product has been tested against Landsat scenes with 900 m^2 spatial resolution, resulting in an average correlation of 0.8 (J. M. N. Silva, personal communication). Only the months of August and September are presented in this study. Individual fires are analyzed by extracting contiguous burned area pixels from each monthly image of burned area. Pixels are considered to be part of the same fire if they were either directly adjacent or connected through any shared corner. No pixels are found to have burned in both the August and September burned area products.

2.2. Fuel Load Product (*F*)

[13] Fuel load is defined as the sum of available fuels. African savanna fires are predominately surface fires, so only grass, litter, and small woody debris are considered as fuel. The fuel load modeling procedure described by C. Hély et al. (A temporal and spatially explicit primary production model for fuel load allocation over the southern African region, submitted to *Journal of Ecological Modelling*, 2002) is used to determine total available fuel during the time period of the SAFARI 2000 dry season intensive. The model calculates fuel availability at 1 km^2 resolution over the region. Primary productivity is based on a spatially explicit Production Efficiency Model parameterized for use in an African savanna [*Dowty*, 1999]. The model takes into account grass growth and death as well as tree litterfall, twig production, and herbivory. The fuel load model has been tested for the 1991–1992 and 1999–2000 growing seasons [*Hély et al.*, 2002a], which represent two climatically contrasting years. These tests have shown good agreement with independent field measurements [*Hély et al.*, 2002a]. Previous studies of African fire regimes using coarser burned area data (25 km^2) have found a high percentage of pixels to be burned more than once in a single year [*Barbosa et al.*, 1999]. Based on the use of high-resolution burned area occurrence (1 km^2) this study assumes that no pixels burned in August and September 2000 had burned previously in the same year. Therefore, the total fuel load available for burning at the end of August 2000 is determined by accumulating fuel load throughout the period of September 1999 to August 2000.

2.3. Combustion Completeness (*CC*)

[14] Other than the direct effect of prevailing weather conditions, combustion completeness (*CC*) is mainly driven by the fuel type, fuel spatial arrangement, and fuel moisture content, with fine and/or dry fuel presenting higher *CC* than thick and/or moister fuel. Because this study focuses on a 2-month period at the end of the dry season, it is assumed that regional fuels over southern Africa were sufficiently dry to ignore the dependency of *CC* on moisture content. The presence of relatively high fuel load moisture content in August and September 2000 in certain moist infertile grasslands such as "dambos" in Zambia [*Hély et al.*, 2002b] as compared to lower moisture content measured in 1992 during SAFARI-92 in equivalent areas may cast some doubt on the validity of this assumption at local scales. However, these grasslands are restricted to depressed areas near the Zambezi river and have minimal impact at regional scales.

[15] *Scholes et al.* [1996b, equation (14)] present an empirical relationship between *CC* and the amounts of each fuel type. This study compares estimates derived from that relationship and a new empirical relationship between *CC* and tree cover percentage (T_c). The use of percent tree cover to calculate combustion completeness is appropriate because tree cover controls fuel type distribution in the fuel load model, and influences local relative humidity and wind speed [*Schroeder and Buck*, 1970], which both significantly influence *CC* through changes in fire propagation and intensity [*Hoffa et al.*, 1999; *Hély et al.*, 2002b]. Moreover, the approach relating *CC* to percent tree cover has been successfully used in Etosha National Park region of Namibia where S. Alleaume et al. (Using MODIS to evaluate heterogeneity of biomass burning and emissions in southern African savannas: Etosha National Park case study, submitted to *International Journal of Remote Sensing*, 2002, hereinafter referred to as Alleaume et al., submitted manuscript, 2002) derived an empirical relationship between *TC* and *CC* in order to estimate the emissions released for a unique fire event that burned 3200 km^2 in approximately 12 days. In the present study, data on tree cover and *CC* from Etosha are combined with available data from SAFARI-92 dry season campaign studies [cf. *Shea et al.*, 1996, Tables 1–4]. Tree cover at the SAFARI-92 sites is taken from *Trollope et al.* [1996, Table 7]. The empirically derived relationship between *CC* and percent tree cover (T_c) is:

$$\begin{aligned} T_c \le 60 \quad & [CC]_{ij} = \exp\left(-0.013 \cdot [T_c]_{ij}\right) \\ T_c > 60 \quad & [CC]_{ij} = 0.3 \end{aligned} \tag{8}$$

[16] The resulting relationship provides an r^2 of 0.54 (n = 32, F = 36.47, $p < 0.0001$), which is a slight improvement over the relationship provided in *Scholes et al.* [1996a] (r^2 = 0.48). However, there is still considerable uncertainty in these estimates that is likely related to changing weather conditions occurring during fires as noted by *Scholes et al.* [1996a], as well as to the land use type [*Shea et al.*, 1996]. The *CC* relationship presented here is sensitive to changes in vegetation structure with *CC* bounded by an upper limit of 1.0 at sites where grass is the only fuel type available (i.e., $T_c = 0$), and by a lower limit of 0.3 in closed canopy stands where the dominating fuel types are litter and twigs (Alleaume et al., submitted manuscript, 2002). In contrast, the relationship defined in *Scholes et al.* [1996a] allows *CC* to range from 0.98 to less than 0.01 over the range of fuel loads predicted (from 0 to $\sim$1000 g m^{-2}). Published values for minimum *CC* are approximately 0.4 in several regional field studies [*Ward et al.*, 1992; *Shea et al.*, 1996; *Hoffa et al.*, 1999; *Hély et al.*, 2002b]. Therefore, the lower limit of 0.3 is assumed to be more realistic, as fires with lower combustion completeness values would be difficult for remote sensing platforms to detect, and sustained burns with combustion completeness values less than 0.3 would be increasingly unlikely.

2.4. Emission Factors (*EF*)

[17] Emission Factors are taken from *Ward et al.* [1996a, 1996b] as these data are the most reliable values currently

Table 1. Empirical Compound-Specific Slopes (α_x) and Intercepts (β_x) Used to Define the Relationship Between Combustion Efficiency ($\hat{\eta}$) and EFs (EF_x) Recalculated From the Studies of *Ward et al.* [1996, 1996b][a]

EF_x [g x/kg fuel]	β_x [g x/kg fuel]	α_x [g x/kg fuel]	n	p	r^2
EF_{CO_2}	−278.131 (47.384)	2118.306 (50.716)	13	<0.0001	0.994
EF_{CO}	1154.466 (13.919)	−1154.707 (14.898)	13	<0.0001	0.998
EF_{CH_4}	60.798 (7.692)	−62.448 (8.232)	13	<0.0001	0.840
EF_{NMHC}	45.519 (5.433)	−45.814 (5.811)	5	<0.005	0.954
$EF_{PM<2.5}$	87.540 (25.843)	−88.405 (27.714)	10	0.01	0.560

[a]Value in parentheses represents the standard error associated to the estimate.

available for late dry season fires in southern Africa. The relationship for each *EF* is recalculated based on the data presented by *Ward et al.* [1996a, 1996b, Tables 1 and 3] to remove errors in their regression equations. The emission factor for each compound (CO_2, CO, CH_4, NMHC and $PM_{2.5}$) is derived using the modified Combustion Efficiency ($\hat{\eta}$), which is the ratio of CO_2 to the sum of CO + CO_2 [*Ward et al.*, 1996a, 1996b]. The $\hat{\eta}$ is determined for each pixel using the ratio of grass fuel load (F_{GRASS} [g m^{-2}]) to the sum of litter (F_{LITTER} [g m^{-2}]) and grass fuels present before the fire using the following recalculated equation (n = 13; F = 46.66; p < 0.0001; r^2 = 0.7954).

$$[\hat{\eta}]_{ij} = 0.844 + 0.116 \times \left(\frac{[F_{GRASS}]_{ij}}{[F_{GRASS}]_{ij} + [F_{LITTER}]_{ij}} \right)^{0.34} \quad (9)$$

[18] The resulting value of $\hat{\eta}$ is used in a linear regression with compound-specific slope (α_x) and intercept (β_x) parameters to determine EF_x according to (4), with compound-specific parameters and the regression parameters provided in Table 1.

$$[EF_x]_{ij} = \alpha_x \cdot [\hat{\eta}]_{ij} + \beta_x \quad (10)$$

2.5. Analyses

[19] Statistics of regional estimations for the fuel load, CC, and area burned in August and September 2000 are presented in Table 2. Statistics only include pixels covered by vegetation. When comparing the two CC approaches based on vegetated pixels (not shown here), the average difference between the two CC approaches is null, 31.4% of the pixels present absolute difference less than 10%, and 56.4% of the pixels show difference less than 20%. Among the 18,807 fires that were detected by SPOT-VGT-S1 in August, approximately 6500 fires are 1 km^2 in size, while only one fire event of >3500 km^2 occurred. September data present the same pattern but with only 12,260 fires detected. Emissions of CO_2, CO, CH_4, NMHC, and $PM_{2.5}$ over southern Africa are estimated for August and September 2000 by applying (1) and (2). Values of total emissions for each trace gas and aerosol component are calculated over the entire region, and according to latitude using latitudinal bands of 5°. The contribution of emissions provided by each fire is used to generate scale-specific estimates of emissions from fires. The cumulative distribution of emissions by fire scale is compared to the cumulative distribution of burned area by fire scale. Finally, an analysis of the ratio between carbon emissions and carbon in consumed biomass is presented.

3. Results

3.1. Emissions Released During the SAFARI 2000 Dry Season Campaign

[20] Total emission estimates of CO_2, CO, CH_4, NMHC, and $PM_{2.5}$ over the southern African region from biomass burning during the August and September 2000 period and using two different *CC* calculations are reported in Table 3 in association with literature data from previous years. The two relationships to calculate *CC* produce very similar emission estimates, with the maximum difference between both at the regional level being 4.2% for CO_2 estimates in August, while the minimum difference is 1.5% for CH_4 estimates in September 2000.

[21] The latitudinal distribution of emissions during August and September from the equator to 35°S is presented in Figure 1. All gases present the same spatial pattern of emission distribution for a given month, with maximums occurring between 5°S and 15°S in August 2000, and between 10°S and 20°S in September. In addition, emission estimates for all gases decrease between August and September over 5°–15°S, whereas they are similar over the other latitudes. Taken together, these patterns are consistent with previous analyses of burning in the region during August and September [*Scholes et al.*, 1996b; *Hao et al.*, 1990; *Justice et al.*, 1996], which found August to be the period of highest emissions, with most burning confined to 5°–20°S latitude.

3.2. Emissions Versus Fire Size

[22] Because the relationships between fire size and emissions are consistent across compounds and between

Table 2. Statistics of Regional Estimations for the Fuel Load Distribution, Combustion Completeness (*CC*), CO_2*EF* (EF_{CO_2}), Fire Size, and Total Burned Area in August and September 2000

Variable	Total Fuel Load (g m^{-2})	CC Calculated From (8)	CC According to the Study of *Scholes et al.* [1996a]	EF_{CO_2} (g kg^{-1}) Calculated From Revised Equation Presented in Table 1	SPOT- Fire Size in Aug. 2000 (km^2)	SPOT-Fire Size in Sept. 2000 (km^2)
Mean	351	0.694	0.644	1576.7	8.63	7.83
Standard Deviation	137.6	0.214	0.249	101.3	45.7	33.9
Min	3	0.3	0.007	N/A	1	1
Max	1311	1	0.983	N/A	3535	1458
N fires					18,807	12,260
Total Burned Area					162,328	95,962

Table 3. Emission Estimates of CO_2, CO, CH_4, NMHC, and $PM_{2.5}$ (in 10^{12} g) Derived From Biomass Burning Over Subequatorial Africa During August and September 2000 Using Two Different *CC* Relationships as Well as Estimates From Previous Studies

	2000 S2K-DSI Emissions[a] (8)			2000 S2K-DSI Emissions[b] (*Scholes et al.* [1996a] equation)			SAFARI-92 Estimates [*Scholes et al.*, 1996b][c]	Other Estimates
	Aug.	Sept.	Total	Aug.	Sept.	Total		
CO_2	59.31	37.63	96.94	64.48	40.09	104.57	136.08	271.6[d]; 92.8[e]
CO	2.89	1.72	4.61	2.98	1.73	4.71	6.30	3.679[e]
CH_4	0.099	0.057	0.156	0.099	0.055	0.154	0.21	0.103[e]
NMHC	0.105	0.062	0.167	0.107	0.062	0.169		
$PM_{2.5}$	0.192	0.113	0.305	0.196	0.113	0.309	0.45	

[a]Emissions derived using the Tree cover and *CC* relationship defined in (8).
[b]Emissions derived using the relationship defined by *Scholes et al.* [1996a].
[c]According to *Scholes et al.* [1996b, Figure 1], total emissions during August and September for CO represent 40% of the total CO emitted over the year 1989. We used this percentage to compare the *Scholes et al.* [1996b, Table 2] estimations with those presented here for subequatorial Africa.
[d]For a 2-month period during the fire season according to *Hao et al.* [1990, Figure 1b] by doubling mean monthly CO_2 emissions for subequatorial Africa.
[e]For 2 months according to *Scholes and Andreae* [2000, Figure 4] by using 40% of the yearly emissions for subequatorial Africa.

the 2 months used in this study, analysis of fire size and emissions is presented using only CO_2 emissions from August fires (Figure 2). The variability in emissions from individual fires decreases as a function of fire size (Figure 2a). Emissions of CO_2 from individual 1 km^2 fires span 3 orders of magnitude (10^6–10^9 g km^{-2}), while larger fires tend to exhibit less variability. This is likely due to the spatial averaging of the variability in both fuel load and combustion completeness (Table 3). The sum of emissions produced by individual fires at each fire size is most heavily weighted toward smaller fires (Figure 2b). Emissions from 2 km^2 fires represent the single largest contribution of emissions, with 2.66 Tg produced, or 4.5% of the total CO_2 emissions during August. Although individual small fires exhibit a greater degree of variability in emissions than large fires, the mean amount of emissions per pixel from the smallest (1 km^2) fires is the same as the mean amount of emissions from largest fire (>3500 km^2).

[23] The cumulative percentage of CO_2 emissions as a function of fire size (Figure 3a) shows that 50% of CO_2 emissions in August are released from fires less than 32 km^2 in size. Although fires less than 32 km^2 represent 96% of the total number of fires observed in August, their contribution to total burned area is only 49% (Figure 3b). The distribution of cumulative percent emissions as a function of fire size (Figure 3a) and cumulative burned area as a function of fire size (Figure 3b) are found to be statistically indistinguishable (Figure 3c). No bias is found in the fuel load and combustion completeness across fire sizes, so that on average small fires emit the same quantity of emissions as large fires on a per pixel basis.

3.3. Mass Balance of Carbon Emissions

[24] In order to assess the mass balance of carbon-bearing emissions predicted from the model, we sum the carbon content of emissions from CO_2, CO, CH_4, and $PM_{2.5}$. Figure 4 provides the relationship between $\sum[EF_x]ij \cdot Mr_x$ and combustion efficiency $\hat{\eta}$. For all possible values of $\hat{\eta}$, the total predicted emissions of carbon are greater than the maximum permissible emissions of 450 g C per kg fuel (cf. (7)). The over estimation of carbon-derived emissions from available carbon in fuel is a persistent problem in published models of compound-specific emission factors. The direct implications on this modeling effort are discussed in the following section.

4. Discussion

[25] In order to assess the utility of our approach it is necessary to compare our results to other estimates of regional emissions. However, because a direct comparison of regional emission estimates for 1999–2000 is currently impossible due to a lack of similar studies, we compare the results provided here with previous estimates for earlier years. Total regional emission estimates are in good agreement with recently published values for 1989 [*Scholes et al.*, 1996a, 1996b; *Scholes and Andreae*, 2000], although larger differences are observed when compared to estimates from 1975 to 1980 (cf. Figure 1 and Table 3) [*Hao et al.*, 1990]. The latitudinal distribution of CO emissions over the course of the 1989 dry season presented by *Scholes et al.* [1996b] is similar to patterns presented in the present study (Figure 1), with the exception of the 0°–5°S latitude band.

[26] Although differences in yearly rainfall are likely to modify fuel load, variability in burned area is the primary reason for yearly variability in emissions. Indeed, in a comparison of 2 years with contrasting rainfall, *Hély et al.* [2002a] have shown the effect of different rainfall amounts on fuel load is limited to the local scale. Furthermore, previous studies have noted the dependence of regional emissions on burned area [*Barbosa et al.*, 1999]. In this study, the high degree of correlation between the cumulative distribution of burned area by fire size and cumulative distribution of CO_2 emissions by fires size in August (Figure 3) reinforces the oft-repeated observation that estimates of emissions in southern Africa are dominated by estimates of burned area. The 40% decrease in total area burned from August to September (see Table 2) corresponds a 47% decrease in CO_2 and 40% decrease for the others gas and aerosol compounds. This trend in monthly change has been reported by *Scholes et al.* [1996b, Figure 1]. The seemingly scale-independent relationship between burned area and total emissions over southern Africa is a subject that requires more detailed investigation. These results suggest that previously given arguments on the reliability of emission

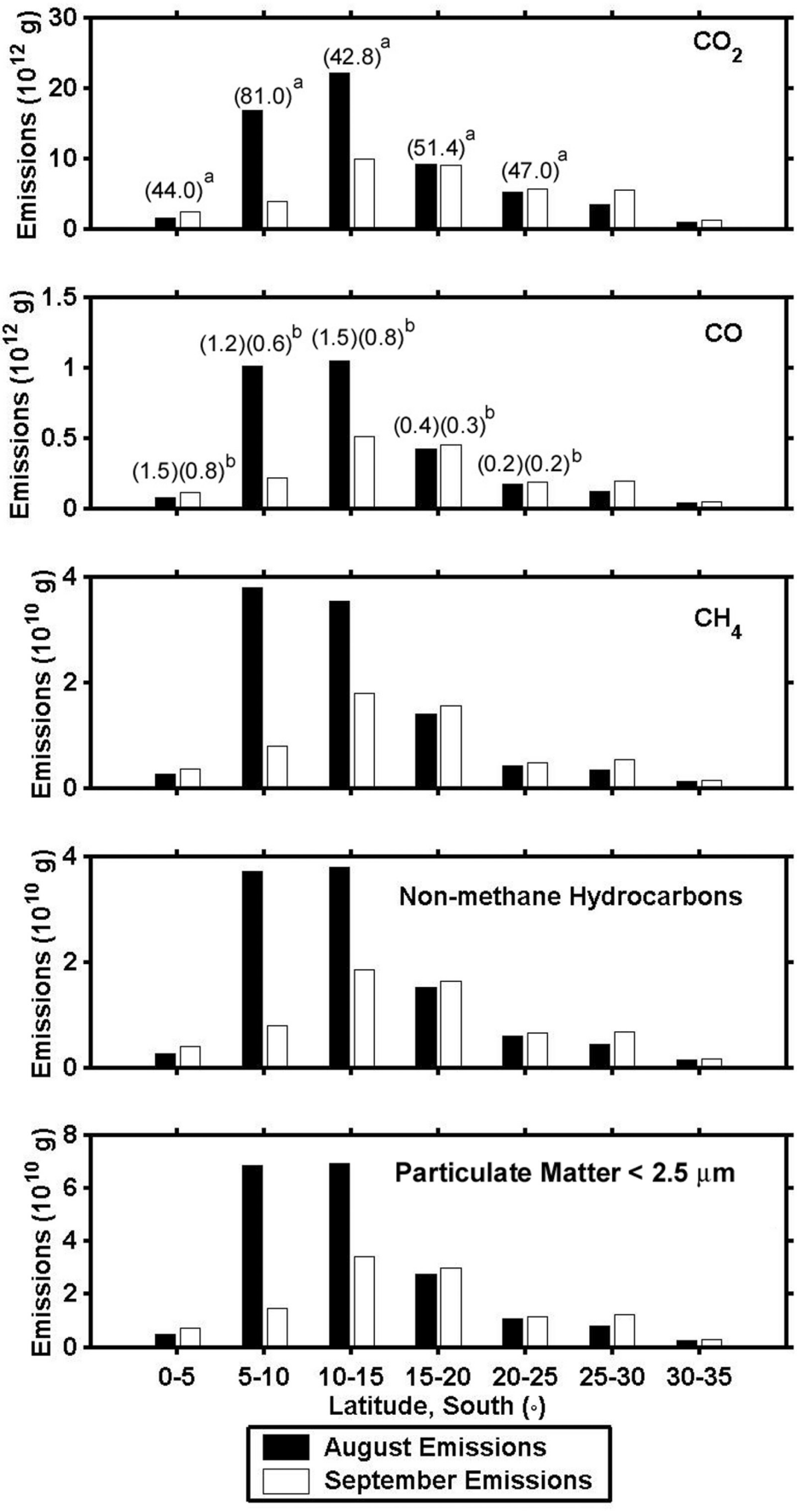
Emissions (10^{12} g)
30
20
10
0
CO_2
(44.0)[a]
(81.0)[a]
(42.8)[a]
(51.4)[a]
(47.0)[a]
Emissions (10^{12} g)
1.5
1
0.5
0
CO
(1.5)(0.8)[b]
(1.2)(0.6)[b]
(1.5)(0.8)[b]
(0.4)(0.3)[b]
(0.2)(0.2)[b]
Emissions (10^{10} g)
4
2
0
CH_4
Emissions (10^{10} g)
4
2
0
Non-methane Hydrocarbons
Emissions (10^{10} g)
8
6
4
2
0
Particulate Matter < 2.5 μm
0-5
5-10
10-15
15-20
20-25
25-30
30-35
Latitude, South (◦)
August Emissions
September Emissions

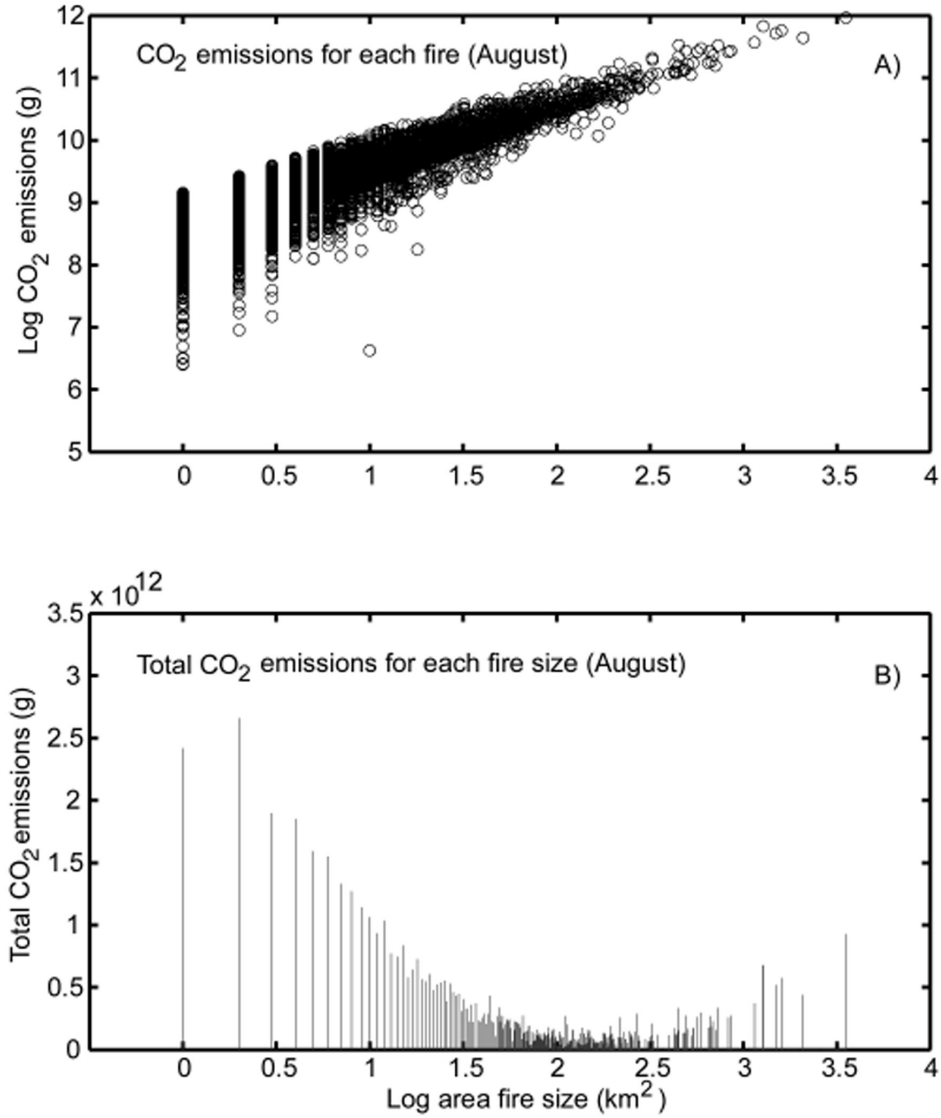

Figure 2. Distribution of CO_2 emission estimates by fire size for individual fires observed during August 2000 (a) and total CO_2 emissions by fire size for August 2000 (b).

estimates based on biomass burning (load and combustion completeness) were less pertinent than those based on the area burned estimates.

[27] As noted above, the emissions model used here depends on emission factors that consistently predict emissions in excess of the amount of carbon contained in the fuel (Figure 4). This is a direct result of the currently implemented modeling approaches that relate compound-specific emission factors to combustion efficiency. Indeed, when field-derived compound-specific emissions factors from multiple fires are used in empirical modeling approaches, the implied mass balance constraints associated with emission factors derived from an individual fire are ignored, and factors are allowed to vary independently. In addition, compound-specific emission factors (EF_x) always relate emissions of a compound (E_x) to total burned biomass (B), without any specific checks on total carbon mass burned (M_C) (cf. (1), (3), and (4)). We report the discrepancy between E_C and M_C in order to highlight the danger in applying linear regressions between emission factors and combustion efficiency (cf. (10)) over regional areas and across wide ranges of combustion efficiencies.

Figure 1. (opposite) Latitudinal distribution of biomass burning emissions estimates by compound for subequatorial Africa during August and September 2000. [a]Data taken from the study of *Hao et al.* [1990, Figure 1b]. Values represent mean cumulative CO_2 emissions for 2 months in the fire season during the period 1975–1980. [b]Data for 1989 taken from the study of *Scholes et al.* [1996b, Figure 1].

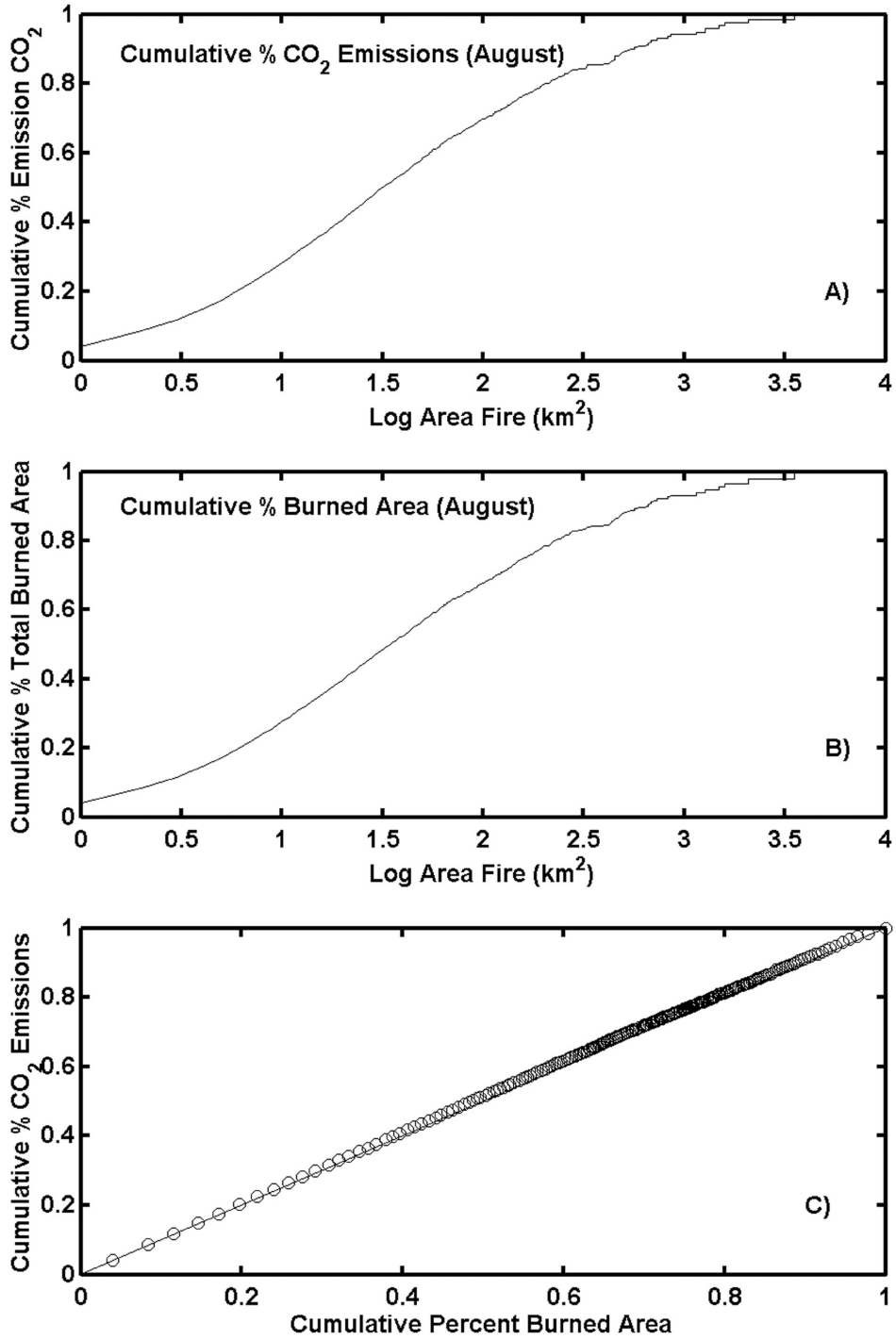

Figure 3. Cumulative percent distribution of CO_2 emissions during August 2000 as a function of fire size (a), cumulative percent distribution of total burned area by fire size (b), and a scatterplot of the two cumulative distributions, with 1:1 line provided (c).

[28] It should be noted that the GBA2000 product from SPOT-VGT-S1 is the only currently available burned area product for use during the 2000 fire season over southern Africa. Trends that have been extracted from this product may suffer from the lack in finer spatial resolution. Indeed, fires that are predominantly ignited by humans for agricultural purposes are generally smaller than the minimum detectable fire size of 1 km^2. The high number of fires detected at 1 and 2 km^2 in size indicates that sub 1 km^2 data, such as the MODIS product when it will become available, will be important in understanding the true role of human activity in controlling the emissions over southern Africa. We expect that the availability of new burned area products from MODIS, as well as analysis of both in situ and derived

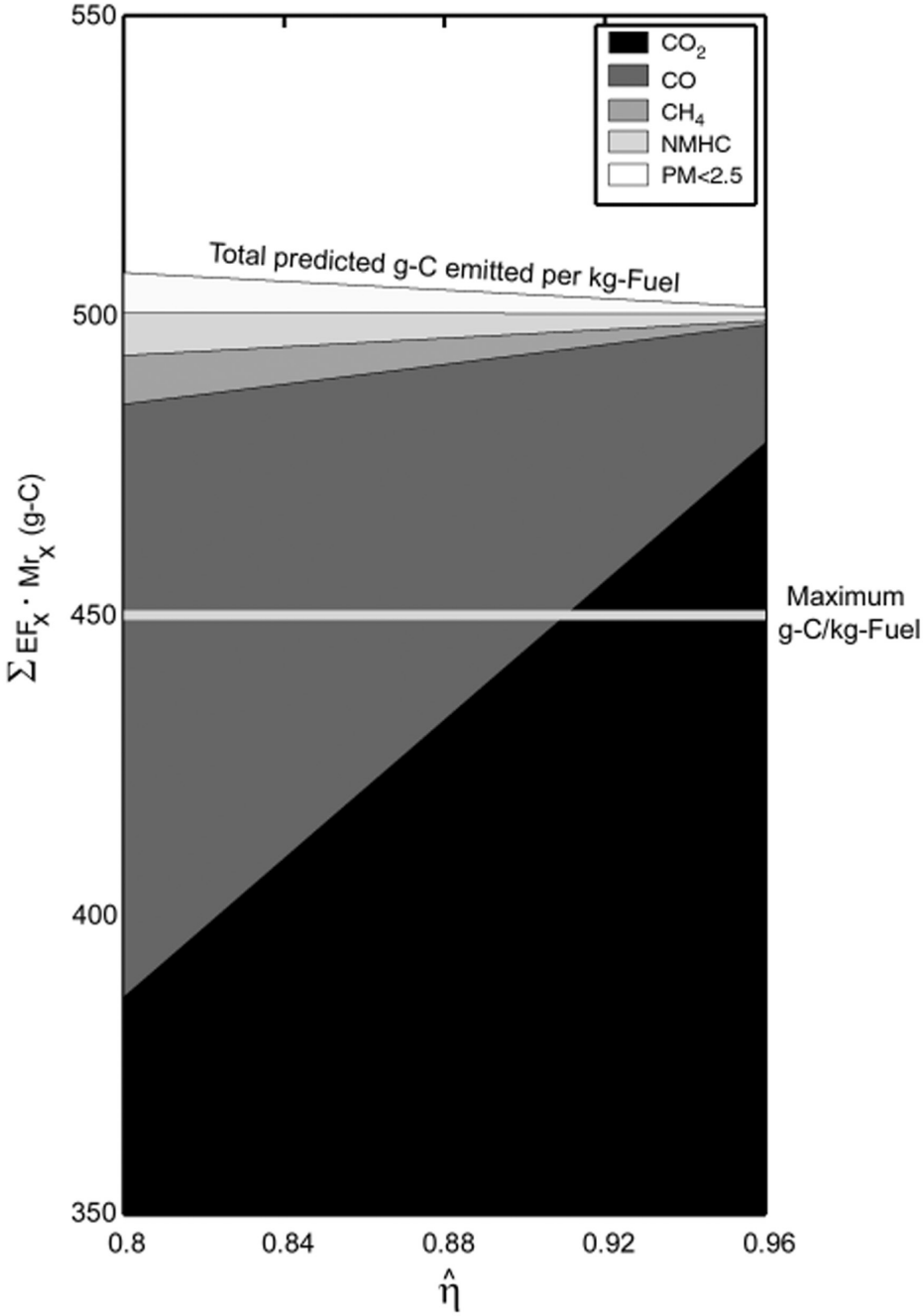

Figure 4. Total predicted grams of carbon emitted ($\Sigma\ EF_x \cdot Mr_x$) as a function of combustion efficiency ($\hat{\eta}$) based on corrected relationships derived from the studies of *Ward et al.* [1996a, 1996b]. The maximum amount of emitted carbon per kg fuel is always assumed to be 450 g. Individual compound contributions are shown and vary in accordance with field observations. However, despite revisions in the empirical relationships (compare (9) and (10), Table 1, [this paper], and Figures 3 and 4 [*Ward et al.*, 1996a, 1996b]), the current *EF* modeling approach still overestimates total carbon emitted by ~10% across all combustion efficiencies.

aerosol products presented elsewhere in this issue will lead to new verification activities.

5. Conclusion

[29] Results presented here provide the SAFARI 2000 community with a first approximation of emission estimates over southern Africa during the 2000 Dry Season Intensive. Total emissions for subequatorial Africa during August and September 2000 are 96.94 Tg CO_2, 4.61 Tg CO, 0.156 Tg CH_4, 0.167 Tg NMHC, and 0.305 Tg $PM_{2.5}$. The spatial progression of these emissions from August to September is consistent with previous observations of biomass burning patterns in southern Africa. Consistency between cumula-

tive percent burned area and cumulative percent emissions suggests that burned area is the primary controlling influence on emission estimates in southern Africa. Any validation or error analysis of the emissions model presented here would be premature given the problems currently facing model-based emission factors and the subsequent overestimation of total emissions. Given the high correlation between emissions and burned area both within this study and in previous studies, it is likely that the greatest source of error in emission estimates is currently burned area. In particular, the detection of small fires is critical, as they constitute almost 5% of the total emissions during the period of August and September 2000. Regardless, the regional values obtained are in agreement with previously published values, and the spatial patterns of emissions correlate well with observed regions of high fire activity.

[30] **Acknowledgments.** This paper was part of the SAFARI 2000 "Southern African Regional Science Initiative." This research was supported by the Southern Africa Validation of EOS program (SAVE-NASA-NAG5-7266), NASA-NAG5-7862, and the InterDisciplinary Science program (IDS-NASA-NAG5-9357). K. K. Caylor was additionally supported by a NASA Earth System Science fellowship.

References

Andreae, M. O., Climatic effects of changing atmospheric aerosol levels, in *World Survey of Climatology, Vol. 16: Future Climates of the World*, edited by A. Henderson-Sellers, pp. 341–392, Elsevier Sci., New York, 1995.

Barbosa, P. M., D. Stroppiana, J.-M. Gregoire, and J. M. C. Pereira, An assessment of vegetation fire in Africa (1981–1991): Burned areas, burned biomass, and atmospheric emissions, *Global Biogeochem. Cycles*, *13*, 933–950, 1999.

Cofer, W. R., III, J. S. Levine, E. L. Winstead, D. R. Cahoon, D. I. Sebacher, J. P. Pinto, and B. J. Stocks, Source compositions of trace gases released during African savanna fires, *J. Geophys. Res.*, *101*, 23,597–23,602, 1996.

Crutzen, P. J., and M. O. Andreae, Biomass burning in the Tropics: Impact on atmospheric chemistry and biogeochemical cycles, *Science*, *250*, 1669–1678, 1990.

Dowty, P. R., Modeling biophysical processes in the savannas of southern Africa, Ph.D. thesis, 228 pp., Environ. Sci., Univ. of Virginia, Charlottesville, Va., 1999.

Fishman, J., K. Fakhruzzaman, B. Cros, and D. Nganga, Identification of widespread pollution in the Southern Hemisphere deduced from satellite analyses, *Science*, *252*, 1693–1696, 1991.

Grégoire, J.-M., K. Tansey, I. Marengo, D. Stroppiana, and S. Fritz, The Global Burnt Area 2000 initiative: GBA-2000: Mapping the areas burnt globally during the year 2000, publications of the Eur. Comm., I.01.117, Joint Res. Cent., Ispra, Italy, p. 40, January 2002.

Hao, W. M., M. H. Liu, and P. J. Crutzen, Estimates of annual and regional releases of CO_2 and other trace gases to the atmosphere from fires in the Tropics, based on the FAO statistics for the period 1975–1980, in *Fire in the Tropical Biota: Ecosystem Processes and Global Challenges, Ecol. Stud.*, vol. 84, edited by J. G. Goldammer, pp. 440–462, Springer-Verlag, New York, 1990.

Hao, W. M., D. E. Ward, G. Olbu, and S. P. Baker, Emissions of CO_2, CO, and hydrocarbons from fires in diverse African savanna ecosystems, *J. Geophys. Res.*, *101*, 23,577–23,584, 1996.

Hély, C., P. D. Dowty, S. Alleaume, K. K. Caylor, S. Korontzi, H. H. Shugart, and C. O. Justice, Regional fuel load for two climatically contrasting years in southern Africa, *J. Geophys. Res.*, *108*, doi:10.1029/2002JD002341, in press, 2002a.

Hély, C., S. Alleaume, R. J. Swap, C. O. Justice, and H. H. Shugart, SAFARI-2000 characterization of fuels, fire behavior, combustion completeness, and emissions from experimental burns in infertile grass savannas in western Zambia, *J. Arid Environ.*, in press, 2002b.

Hoffa, E. A., D. E. Ward, W. M. Hao, R. A. Susott, and R. H. Wakimoto, Seasonality of carbon emissions from biomass burning in a Zambian savanna, *J. Geophys. Res.*, *104*, 13,841–13,853, 1999.

Kuhlbusch, T. A. J., M. O. Andreae, H. Cachier, J. G. Goldhammer, J.-P. Lacaux, R. Shea, and P. J. Crutzen, Black carbon formation by savanna fires: Measurements and implications for the global carbon cycle, *J. Geophys. Res.*, *101*, 23,651–23,665, 1996.

Lindesay, J. A., M. O. Andreae, J. G. Goldhammer, G. Harris, H. J. Annegarn, M. Garstang, R. J. Scholes, and B. van Wilgen, The IGBP/IGAC SAFARI-92 field experiment: Background and overview, *J. Geophys. Res.*, *101*, 23,521–23,530, 1996.

Otter, L. B., et al., The Southern African Regional Science Initiative (SAFARI 2000): Wet season campaigns, *S. Afr. J. Sci.*, *98*, 131–137, 2002.

Pereira, J. C. M., M. J. P. Vasconcelos, and A. M. Sousa, A ruled-based system for burned area mapping in temperate and tropical regions using NOAA-AVHRR imagery, in *Biomass Burning and its Inter-Relationships With the Climate System*, edited by J. L. Innes, M. Beniston, and M. Verstraete, Kluwer Acad., Norwell, Mass., 2000.

Pickering, K. E., A. M. Thompson, D. P. McNamara, and M. R. Schoeberl, An intercomparison of isentropic trajectories over the South Atlantic, *J. Geophys. Res.*, *97*, 7859–7882, 1994.

Piketh, S. J., R. J. Swap, C. A. Anderson, M. T. Freiman, M. Zunckel, and G. Held, The Ben Macdhui High Altitude Trace Gas and Aerosol Transport Experiment, *S. Afr. J. Sci.*, *95*, 35–49, 1999.

Prince, S. D., S. J. Goetz, and S. N. Goward, Monitoring primary production from earth observing satellites, *Water Air Soil Pollut.*, *82*, 509–522, 1995.

Scholes, M. C., and M. O. Andreae, Biogenic and pyrogenic emissions from Africa and their impact on the global atmosphere, *Ambio*, *29*, 23–29, 2000.

Scholes, R. J., Greenhouse gas emissions from vegetation fires in southern Africa, *Environ. Monit. Assess.*, *38*, 169–179, 1995.

Scholes, R. J., J. Kendall, and C. O. Justice, The quantity of biomass burned in southern Africa, *J. Geophys. Res.*, *101*, 23,667–23,676, 1996a.

Scholes, R. J., D. E. Ward, and C. O. Justice, Emissions of trace gases and aerosol particles due to vegetation burning in southern hemisphere Africa, *J. Geophys. Res.*, *101*, 23,677–23,682, 1996b.

Schroeder, M. J., and C. C. Buck, Fire weather: A guide for application of meteorological information to forest fire control operations, USDA For. Serv., Agric. Handb. 360, 229 pp., 1970.

Shea, R. W., B. W. Shea, J. B. Kauffman, D. E. Ward, C. I. Haskins, and M. C. Scholes, Fuel biomass and combustion factors associated with fires in savanna ecosystems of South Africa and Zambia, *J. Geophys. Res.*, *101*, 23,551–23,568, 1996.

Stocks, B. J., B. W. van Wilgen, and W. S. W. Trollope, Fire behaviour and the dynamics of convection columns in African savannas, in *Fire in Southern African Savannas: Ecological and Atmospheric Perspectives*, edited by B. W. van Wilgen, M. O. Andreae, J. G. Goldammer, and J. A. Lindesay, pp. 47–55, Witswatersrand Univ. Press, Johannesburg, S. Afr., 1997.

Swap, R. J., H. J. Annegarn, and L. Otter, Southern African Regional Science Initiative (SAFARI 2000): Summary of science plan, *S. Afr. J. Sci.*, *98*, 19–124, 2002a.

Swap, R. J., et al., The Southern African Regional Science Initiative (SAFARI 2000): Dry-Season Field Campaign: An overview, *S. Afr. J. Sci.*, *98*, 125–130, 2002b.

Trollope, W. S. W., L. A. Trollope, A. L. F. Potgieter, and N. Zambatis, SAFAR-92 characterization of biomass and fire behavior in the small experimental burns in the Kruger National Park, *J. Geophys. Res.*, *101*, 23,531–23,539, 1996.

Ward, D. E., R. A. Susott, J. B. Kauffman, R. E. Babbitt, D. L. Cummings, B. Dias, B. N. Holben, Y. J. Kaufman, R. A. Rasmussen, and A. W. Setzer, Smoke and fire characteristics for Cerrado and deforestation burns in Brazil: BASE-B experiment, *J. Geophys. Res.*, *97*, 14,601–14,619, 1996a.

Ward, D. E., W. M. Hao, R. A. Susott, R. E. Babbitt, R. W. Shea, J. B. Kauffman, and C. O. Justice, Effect of fuel composition on combustion efficiency and emission factors for African savanna ecosystems, *J. Geophys. Res.*, *101*, 23,569–23,576, 1996b.

S. Alleaume, K. Caylor, C. Hély, H. H. Shugart, and R. J. Swap, Environmental Sciences Department, University of Virginia, 291 McCormick Road, Charlottesville, VA 22904-4123, USA. (christelle_hely@hotmail.com; ch8se@virginia.edu)